Inhibition of Muscle Force by Vanadate

Gregory J. Wilson,*‡ Sarah E. Shull,‡ and Roger Cooke‡

*Department of Pathology, The University of Sydney, New South Wales 2006, Australia, and the ‡Cardiovascular Research Institute and Department of Biochemistry and Biophysics, University of California at San Francisco, San Francisco, California 94143-0524 USA

ABSTRACT Vanadate (V_i), an analogue of inorganic phosphate (P_i), is known to bind tightly with a long half life to the myosin MgATPase site, producing a complex which inhibits force. Both of these ligands bind to an actin·myosin·ADP state that follows the release of P_i in the enzymatic cycle, and their effects on muscle fibers and on proteins in solution provide information on the properties of this state. The inhibition of active force generation began to occur at a $[V_i]$ of 5 μM and was 90% complete at a $[V_i]$ of 1 mM. Hill plots of the inhibition of force by V_i approximated that expected for a simple binding isotherm. Similar plots were obtained at both 25°C and 5°C. A simple binding isotherm is not expected to occur in a muscle fiber where steric constraints imposed by the intact filaments should introduce more complexity into the energetics of ligand binding. The inhibition of MgATPase activity for acto-subfragment-1 to 50% of controls occurred at a $[V_i]$ which was only 20-fold higher than that required to inhibit force generation in fibers to the same level. Some models of actomyosin interactions would predict that the range of $[V_i]$ required for complete force inhibition in fibers and the difference in the $[V_i]$ required for inhibition in fibers and of myosin in solution would both be much larger.

INTRODUCTION

Generation of force in active muscle fibers results from the cyclic interaction between actin, myosin, and MgATP. This interaction has been extensively studied, both in solution using purified proteins and in muscle fibers (for reviews see Taylor, 1979; Sleep and Smith, 1981; Cooke, 1986; Hibberd and Trentham, 1986; Goldman and Brenner, 1987; Geeves, 1991). Studies performed in solution have identified a number of the states involved in the cycle, their energetics, and the kinetics of the rates which connect them. These studies have shown that ATP enters the cycle by binding to a strong actomyosin rigor complex, dissociating myosin from actin (Lymn and Taylor, 1971). ATP is subsequently cleaved while myosin is either dissociated from or weakly bound to the actin filament. Release of phosphate (P_i) results in the transition to a more strongly bound actin·myosin·ADP state, which is thought to be the state that is responsible for a majority of the force produced or work performed in active muscle fibers. A similar cycle is presumed to occur in fibers. However, the energetics of the states and the rates between them are thought to be altered by the fact that the proteins are sterically constrained by the filament lattice of the muscle fiber (for reviews see Hibberd and Trentham, 1986; Goldman and Brenner, 1987).

One method of studying the energetics of the actomyosin interaction is to observe the perturbations in this interaction caused by raising the concentration of P_i, one of the products released during ATP hydrolysis. An increased $[P_i]$ lowers the free energy of those states that precede P_i release relative to those states that follow (Pate and Cooke, 1989a, b). Subsequent perturbations observed upon raising $[P_i]$ depend strongly on the properties of the actin·myosin·ADP state to which P_i is binding. The energetics of this state (or states) is of particular interest because of its proposed role in the generation of force. Additional information on the steric constraints imposed by the filament lattice can be obtained by comparing the results obtained in solution with those obtained in fibers.

The effects upon force generation of both P_i and vanadate (V_i), an analogue of P_i, have been previously studied. White and Thorson (1972) were the first to show that P_i had a profound influence on the oscillatory behavior of fibers from insect flight muscles. Subsequent work by a number of laboratories with vertebrate striated muscle showed that P_i decreased tension while having little effect on the fiber contraction velocity (Pate and Cooke, 1989b). The decrease in tension was proposed to result from the reversal from a strongly bound, force-producing actin·myosin·ADP state to a weakly bound, non-force-producing actin·myosin·ADP·P_i state (Hibberd et al., 1985). Mathematical models of muscle cross-bridge function based on this kinetic scheme predicted that tension should depend linearly on the $\log_{10}[P_i]$ and this was in fact observed (Pate and Cooke, 1989a, b; Millar and Homsher, 1990). V_i was found to inhibit the MgATPase activity of myosin (Goodno, 1982). It also inhibited force generation in skinned muscle fibers (Goody et al., 1980; Herzig et al., 1981; Dantzig and Goldman, 1985; Fuchs, 1985; Chase et al., 1993; Pate et al., 1994). Since V_i has a significantly higher affinity for myosin than does P_i, tension can be titrated to near 0 with concentrations of V_i that have little effect on ionic strength, allowing a more accurate determination of the dependence of force upon the ligand concentration. V_i has been shown to bind specifically in a stable complex at the myosin active site by photocleavage studies of the myosin

Received for publication 30 March 1994 and in final form 17 October 1994.

Address reprint requests to Gregory J. Wilson, Cooperative Research Centre for Cardiac Technology, Block 4, Level 3, Royal North Shore Hospital, St Leonard's, NSW 2065, Australia. Tel.: 61-2-926-8698; Fax: 61-2-901-4097.

0006-3495/95/01/216/11 $2.00

active site in the presence of V_i (Cremo et al., 1989; Grammer and Yount, 1994), by trapping of fluorescently or paramagnetically labeled nucleotide analogues to myosin or fibers (Mihashi et al., 1990; Wilson et al., 1990, 1991), and by studies of the competition between V_i and the γ-P_i of ATP for binding to myosin (Werber et al., 1992).

We find rather surprisingly that the inhibition of fiber tension by increased $[V_i]$ follows approximately the behavior expected for the binding of a ligand to a single enzyme site. Full inhibition of the activity is achieved over a range of $[V_i]$ spanning approximately $10^{2.8}$- to $10^{3.0}$-fold. The same behavior is found at two different temperatures, at two different concentrations of P_i, and at a concentration of AlF_x that inhibits force by 75%; yet both temperature and the two ligands should affect the energetics of the actin-myosin interaction, and change the interaction with V_i. Thus, none of the complexity that might be thought to be introduced by the interplay between the steric constraints of the fiber lattice and the energetics for the actomyosin states is evident in the inhibition of force by V_i. This suggests that the binding of V_i involves transitions between states whose relative free energy is independent of the steric constraints imposed by the filament lattice. It appears that the inhibition of force by P_i may follow a similar dependence upon concentration range as that observed for V_i (although the data are not as complete because of constraints brought about by large increases in ionic strength at high $[P_i]$ and because of the difficulties with obtaining very low $[P_i]$ in fibers during the generation of P_i from MgATP hydrolysis). These data thus suggest that the release of P_i is also not directly coupled to the transition to a force-producing state. The transition from low-force to high-force states must be a protein isomerization that occurs before or subsequent to P_i release. An isomerization was also invoked to explain the tension transients that follow the release of caged phosphate in muscle fibers (Dantzig et al., 1992; Walker et al., 1992). A second observation also suggests the presence of a low-force state following P_i release. Steric constraints of the fiber lattice only alter the $[V_i]$ required to inhibit the actomyosin interaction by a factor of 20 compared with that needed for contractile proteins in solution, suggesting the presence of a weakly bound, non-force-producing actin·myosin′·ADP state. A similar state was also proposed earlier to explain the incorporation of labeled P_i into ATP during the hydrolysis cycle (Sleep and Hutton, 1980; Sleep and Smith, 1981; Bowater and Sleep, 1988), and to explain the kinetics of the actomyosin interaction observed in solution (Geeves, 1991; Taylor, 1991). Together the results suggest that the energetics of the transition involved in the binding of V_i are not very sensitive to the constraints generated by the geometry of the filament array.

MATERIALS AND METHODS

Muscle fibers were obtained from rabbit psoas (fast-twitch) muscles. The fibers were then chemically skinned by glycerination as described previously (Cooke et al., 1988; Pate et al., 1994).

Fiber mechanical measurements

The mechanical properties of muscle fibers were measured similarly to previously described methods (Cooke et al., 1988; Pate and Cooke, 1989b; Stephenson et al., 1989; Pate et al., 1994). A sensitive solid state force transducer detected force generation (AME 801, Aksjelskapet, Horten, Norway). Force was monitored using an IBM PC/AT interfaced to the transducer by an analog/digital board (Tecmar, OH). The force baseline was maintained by a feedback loop and the program used to collect data was written in PC/FORTH (Version 3.2, Laboratory Microsystems, CA), as previously described (Cooke et al., 1988), with some modifications. The system was capable of taking data at 4 kHz frequency. Fibers were mounted at one end to a glass hook fixed to the transducer and at the other end to a stainless steel peg attached to the beam of a fast motor (General Scanning, MA). For some of the fibers investigated the ends were fixed using gluteraldehyde (Chase and Kushmerick, 1988). This procedure improved the stability of fibers activated at 25°C, allowing more data to be collected from each fiber. The results obtained from these fibers were, however, not significantly different from unfixed fibers, and the data obtained from the two populations has been pooled. Fibers were mounted within a well in which the temperature was regulated by a water jacket and were activated and relaxed by the addition to the well of appropriate solutions. The resonant frequency of the transducer with fibers mounted and immersed in solution was 2.7 kHz. Fiber dimensions were determined using a dissecting microscope (Wild, Heerbrugg, Netherlands). Initial sarcomere lengths were determined by He-Ne laser diffraction to be between 2.4 and 2.6 μm (Cooke et al., 1988; Stephenson et al., 1989; Pate et al., 1994).

Fiber MgATPase activity

Skinned fibers were activated in solutions similar to those used during tensiometer experiments except that no additional P_i was added (see following section). The MgATPase activity of the skinned fibers activated in the presence and absence of V_i was determined using a modified malachite green assay for P_i generation (Kodama et al., 1986). Bundles containing about 4 fibers were isometrically mounted between two stainless steel pegs and immersed in activating and relaxing solutions of different composition in wells containing 25 μl of solution at 23°C. During activation in the presence of V_i, sufficient time (30 s) was always allowed for the formation of the myosin·ADP·V_i complex to reach a steady state, as determined from force measurements (Fig. 1). The fibers were activated in individual wells and then after 1 min were rapidly transferred to a new well for a total cumulative duration of activation of 3 min. The solutions were then assayed for P_i content. The spectrophotometer standards contained the same $[V_i]$ as the experimental solution samples, to account for the fact that V_i, being a P_i analogue, may affect the assay. Controls for baseline MgATPase activity were performed by incubating relaxed fibers, with no added Ca^{2+}, in the absence of V_i. The cumulative results for the amount of P_i produced were plotted against time and the slope of linear regression fits were taken as the rate of P_i production.

To calculate the absolute MgATPase activity of fibers used in the assay (in molecules of MgATP hydrolyzed s^{-1} per myosin head), the protein content of the fibers was determined. Fibers were sonicated after each experiment in a solution of urea (6 M) and the protein content was determined using a Coomassie Brilliant Blue G assay (Sigma, St. Louis, MO). Myosin content was assumed to be 45% of the total fiber protein content (Cooke and Franks, 1978).

Actin-activated MgATPase activity of myosin subfragment-1 (S1)

Actin-activated MgATPase activity of myosin S1 (Taylor, 1979; Margossian and Lowey, 1982) was also determined by a modified malachite green assay (Kodama et al., 1986). The assay was carried out in solutions containing TES (100 mM, pH 7.0, 23°C), ATP (1 mM), $MgCl_2$ (2 mM), with variable concentrations of KCl. In maximally actin-activated controls, KCl

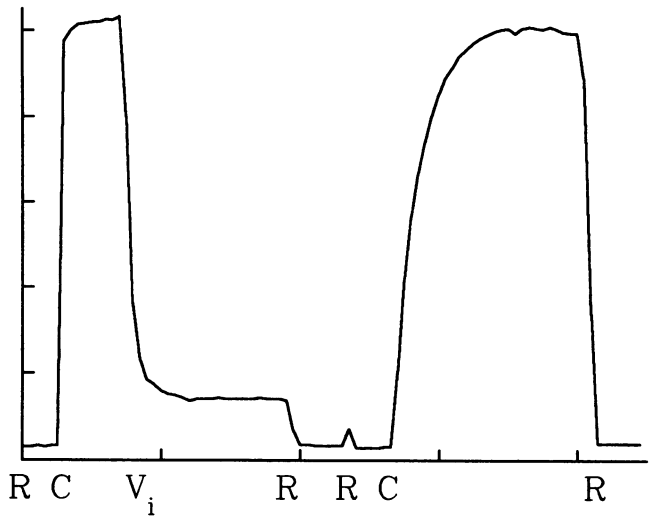

FIGURE 1 Trace showing the protocol used to relax and maximally Ca^{2+}-activate skinned rabbit psoas muscle fibers in the presence of inorganic phosphate (P_i, 5 mM) and vanadate (V_i, 1 mM). The fiber was first relaxed (R) to obtain a baseline. It was then activated by the addition of Ca^{2+} stock solution (C) to give a [free Ca^{2+}] $\geq$ 0.03 mM. V_i stock solution was then added and force generation was allowed to decline to a steady state. The fiber was subsequently relaxed, washed again in relaxing solution, and reactivated. Force generation was again allowed to reach a steady state before the fiber was finally relaxed. The marks along the horizontal axis indicate intervals of 1 min and those along the vertical axis each represent 5 N/cm^{-2} of fiber tension. Data were sampled at the rate of one point every 3 s. Fiber diameter = 65 μm.

(100 mM) was added. Stock V_i solutions were made from $NaVO_3$. Therefore, when V_i was added to the assay solutions to inhibit MgATPase activity, the [KCl] was lowered such that the total ionic strength remained constant. F-actin was prepared from acetone powder (Spudich and Watt, 1971) and was included in the assay at a concentration of 1 mg ml^{-1}. Myosin S1 was prepared from myosin either by papain digestion (Cooke, 1972) or chymotryptic digestion (Weeds and Taylor, 1975) and was included in the assay at a concentration of 18 μg ml^{-1}.

Fiber activation

The composition, pH and ionic strength of the solutions used during fiber relaxation and activation were determined from standard binding constants using a Fortran computer program (Pate and Cooke, 1989b). The solution used for relaxing (and activating) muscle fibers comprised $MgOAc_2$ (5 mM), TES (100 mM), ATP (4 mM total), EGTA (1 mM) and K_2HPO_4 (5 or 50 mM). Experiments were performed at either 5°C or 25°C, and the above buffer was set to pH 7.0 at the appropriate temperature (Pate et al., 1994). An ATP regenerating system was used which consisted of creatine phosphate (20 mM) and creatine phosphokinase (1 mg ml^{-1}). Sufficient KOAc was added to bring the ionic strength to 210 mM. To make an activating solution, calcium ions were added to the relaxing solution as $CaCl_2$ from a stock solution so that the final [free Ca^{2+}] of the activating solutions was $\geq$0.03 mM. Care was taken to ensure that all fibers were fully activated.

Vanadate solutions

Stock solutions of sodium metavanadate ($NaVO_3$, V_i) (EM Science, NJ) of ~100 mM were made. The [V_i] of the stock solution was determined by measuring the absorption at 265 nm, assuming an extinction coefficient of 2925 $M^{-1}cm^{-1}$ (Goodno, 1982). The chemistry of vanadium in aqueous solution is complex (Rubinson, 1981; Penningroth, 1986; Gresser et al., 1986). Therefore consideration must be given to the nature of the vanadium compounds present during these experiments.

Vanadium was present mostly in the V^v oxidation state. Therefore the predominant ionic vanadium species present at pH 7, our experimental pH, would have been the metavanadate ion, VO_3^-. There will also be a small amount of pyrovanadate, HVO_4^{2-} (Rubinson, 1981). At concentrations of greater than 1 mM in the pH range 4–8, the V^v form of vanadium forms polymers. This process is very slow and can be observed by the appearance of a yellow or orange color in the solution (Rubinson, 1981; Goodno, 1982; Penningroth, 1986). For this reason, references in the text to the concentration of V_i can more accurately be interpreted as the total concentration of vanadium atoms.

Stock vanadate solutions were raised to pH 10 to reduce the extent of polymerization during storage. To hydrolyze polymerized species, the solution was always boiled before being used. This procedure eliminated any yellow or orange color caused by polymerization (Rubinson, 1981; Goodno, 1982; Penningroth, 1986). Since it was necessary to store V_i stock solutions at pH 10, high concentrations of pH buffer were needed to compensate for pH changes when V_i was added to the fiber activating solutions. For this reason the [TES] was 100 mM in all activating solutions. When V_i was added to fiber activating solutions in concentrations up to 15 mM from stock V_i solutions at pH 10, increases of not more than 0.1 pH unit were observed. No yellow coloration was observed within the course of the experiments. Since physiological processes were found to be linear over a wide range of [V_i] (Figs. 2–6), this suggests that only one active form of V_i was present in a stable concentration.

P_i and V_i are thought to bind to the same site on the myosin head (Goodno, 1982; Dantzig and Goldman, 1985; Cremo et al., 1989; Wilson et al., 1990; Grammer and Yount, 1994). The concentration of P_i is difficult to regulate within fibers because of diffusional constraints and the constant generation of P_i from myosin MgATPase activity (Kentish, 1986; Pate and Cooke, 1989b; Millar and Homsher, 1990). We therefore included P_i (5 mM) in the activating solutions so that any increase in [P_i] due to MgATPase activity would be small in proportion to the total [P_i]. Therefore changes in fiber mechanics due to V_i would not be masked by changes in the [P_i] within the fibers. However, it is likely that in the presence of P_i some of the active form of V_i was in equilibrium with a covalently bound phosphate/vanadate anhydride (Gresser et al., 1986). Therefore the concentration of the active form of V_i would be altered when the [P_i] is altered, as was the case for the experiments in which we investigated the competition between P_i and V_i for the myosin active site shown in Fig. 2. Therefore, using equilibrium constants for the formation of the phosphate/vanadate anhydride at pH 7 (Gresser et al., 1986), adjustments were made for the concentrations of the active form of V_i present in the activating solutions containing different [P_i] during these experiments. This shifted the curve for the inhibition of force in the presence of 5 mM P_i by 0.04 $\log_{10}$[V_i] units to the left and that for the inhibition of force in the presence of 50 mM P_i by 0.30 $\log_{10}$[V_i] units to the left.

RESULTS

Effects of vanadate upon maximally Ca^{2+}-activated force

Vanadate inhibited the ability of skinned rabbit fast-twitch skeletal muscle fibers to generate force. A typical protocol for trapping V_i on the myosin heads of a single fast-twitch muscle fiber and inhibiting force is illustrated in Fig. 1. Fibers were first maximally Ca^{2+}-activated by adding sufficient Ca^{2+} to the relaxing solution bathing the fiber to give a free [Ca^{2+}] $\geq$ 0.03 mM. When force generation had reached a steady state, V_i from the stock solution was added to the fiber solutions in various concentrations. Force generation was then allowed to decline to a steady state. The half time ($t_{1/2}$) to steady state inhibition was ~5 s for the fiber in Fig.1, where trapping occurred in the presence of a [V_i]

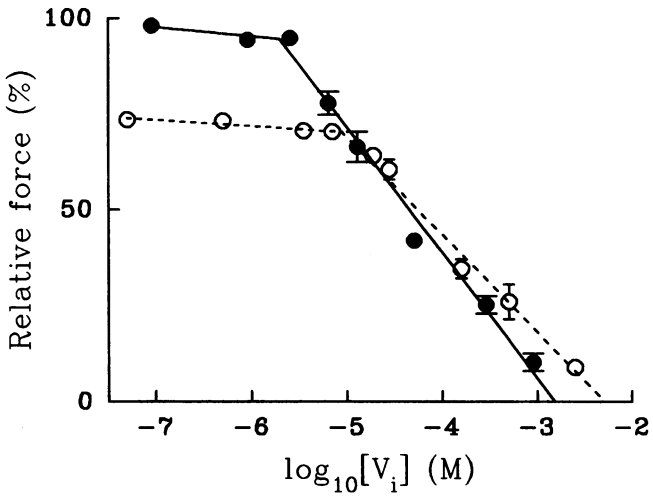

FIGURE 2 Competition between V_i and P_i during inhibition of force simultaneously by both ligands. Plot shows relative maximally Ca^{2+}-activated isometric force vs. $\log_{10}[V_i]$ for fast-twitch skinned rabbit psoas muscle fibers at 25°C in the presence of MgATP (4 mM) and $[P_i]$ of either 5 mM (●) or 50 mM (○). Relative force was determined by comparing the force obtained during activation in the presence of V_i to that obtained either before or after this when fibers were activated in the absence of V_i and in the presence of P_i (5 mM). The bars represent the SEM ($3 \leq n \leq 8$ fibers for each data point). The correlation coefficient for the line of best fit to the data for 5 mM P_i at $[V_i] \geq 3$ μM was $r = 0.98$ and that for data collected in the presence of 50 mM P_i at $[V_i] \geq 17$ μM was $r = 0.99$.

of 1 mM and a $[P_i]$ of 5 mM at 25°C. These effects of V_i were reversible. When fibers were relaxed and then activated again in the absence of V_i, force generation recovered. The $t_{1/2}$ to maximal force recovery during the second activation was ~8.5 s for the fiber in Fig. 1, measured from the time when the force had reached the level to which it was initially inhibited.

Competition between P_i and V_i

When P_i and V_i were included simultaneously in the activation medium, these two ligands competed for the same site on myosin (Werber et al., 1992). In the presence of 5 mM P_i, force remained fairly stable until the $[V_i]$ reached about 2 μM, at which point it began to decline linearly with the $\log_{10}[V_i]$ (Fig. 2). The $[V_i]$ at which maximally Ca^{2+}-activated force was reduced to 50% was ~45 μM. Similarly to this, data from Dantzig and Goldman (1985) and from Fuchs (1985) give values of ~94 and ~60 μM, respectively, for half force inhibition for the same preparation under similar conditions. These data could be fit by a straight line or by a simple isotherm, which approximates a straight line over much of the range. The difference between these two was not significant, and the data of Fig. 2 are fit by straight lines, while the data shown in Fig. 4 are fit by a simple isotherm. The line of best fit to the data obtained at 5 mM P_i and $[V_i] > 2$ μM in Fig. 2, fitted using a least squares linear regression, intercepted the abscissa (zero force point) at a $[V_i]$ near 1.8 mM. In the data shown in Fig. 2 obtained at 5 mM P_i, force was titrated from maximal to zero levels with an increase in $\log_{10}[V_i]$ units of 3.0 (range, 2.7–3.3, 95% confidence limits). The value of this parameter varied from 2.5 to 3.0 $\log_{10}[V_i]$ units for three different preparations with a mean of 2.8 ± 0.3 $\log_{10}[V_i]$ units (mean ± SEM).

When 50 mM P_i was included in the activating solution, maximal force, which was initially ~75% of that obtained in 5 mM P_i, remained constant until the free $[V_i]$ reached ~9 μM, at which point it began to decline linearly with the $\log_{10}[V_i]$ (Fig. 2). The force did not decline in parallel with the decline caused by V_i in 5 mM P_i, as might be expected from some simple competition models. Instead it declined from maximal to 0% as the $[V_i]$ was increased by 2.9 $\log_{10}[V_i]$ units (range, 2.6–3.2, 95% confidence limits). For fibers activated in the presence of 50 mM P_i, force was reduced to 50% when the free $[V_i]$ reached ~200 μM, while the line of best fit intercepted the abscissa at a $[V_i]$ near 5 mM. The positions of these two curves obtained at different $[P_i]$ were not significantly different from each other within 95% confidence limits; therefore the range of $[V_i]$ needed to completely titrate force to 0 in the presence of 5 mM or 50 mM P_i were similar.

Competition between V_i and AlF_x

Competition between two different ligands, both binding to the same site, can provide additional information on the energetics of the actomyosin states involved in the ligand binding. In the experiments described above, V_i competed with P_i for the site on myosin. However, due to contributions made by P_i to the ionic strength (Pate and Cooke, 1989b), the highest attainable level of $[P_i]$ only inhibits force by 25% relative to that obtained in the presence of 5 mM P_i. It has been shown that AlF_x also acts as a P_i analogue, binding to the myosin site and inhibiting ATPase activity and tension (Werber et al., 1992; Chase et al., 1993). Tension could be completely inhibited by low levels of AlF_x. We inhibited fiber tension to 25–30% of control by addition of 10 mM NaF and 50 μM $AlCl_3$, following the protocols of Chase et al. (1993). The remaining tension was titrated to 0 by adding V_i to the activating solutions containing AlF_x. The range of $[V_i]$ required to titrate tension from its level in the presence of AlF_x and the absence of V_i to close to 0 was identical to that required in the absence of AlF_x (Fig. 3).

The effect of temperature

The inhibition of force by V_i provides a probe of the energetics of the states involved. The strength of the actomyosin bond as well as the force generated by a fiber both decrease with temperature. Changing the temperature from 25°C to 5°C altered isometric tension from 25 ± 5 N/cm² to 10 ± 2 N/cm² (mean ± SEM, $n = 5$). This gives a Q_{10} for force generation over this temperature range of 1.58. This is similar to the value of 1.39 found previously by us over the range 10–30°C (Pate et al., 1994). If the free energies of the states that are involved in the binding of V_i are influenced by the strength of the actomyosin interaction, as would be expected

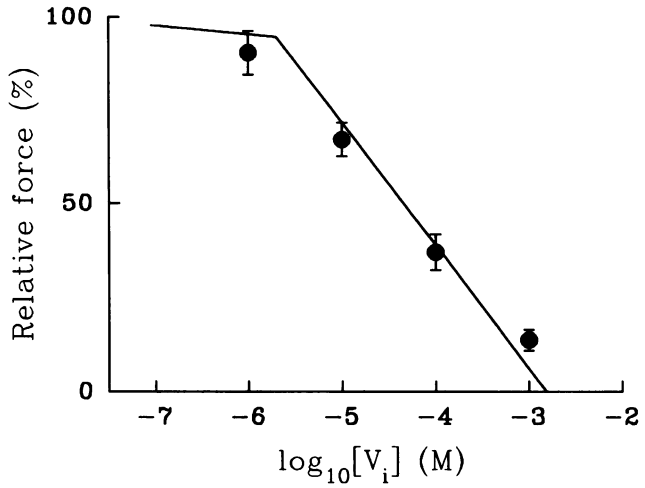

FIGURE 3 Competition between V_i and AlF_x during inhibition of force simultaneously by both ligands. Plot shows maximally Ca^{2+}-activated isometric force vs. $\log_{10}[V_i]$ in the presence of 10 mM NaF and 50 μM $AlCl_3$ at 10°C. Force is normalized to that obtained in the presence of AlF_x and in the absence of V_i. The bars represent the SEM ($3 \leq n \leq 6$ fibers for each data point). The two straight lines are those that were fit to the data obtained in the presence of 5 mM P_i, shown in Fig. 2.

for a state that is involved in the generation of force, then altering the strength of this interaction by lowering the temperature should change the relationship between force and $[V_i]$. To determine whether temperature would influence this relation, the experiment discussed above (Fig. 1) was repeated at 5°C. As shown in Fig. 4, the inhibition of force by V_i follows the same dependence upon concentration as observed at the higher temperature (Fig. 2).

A commonly used method of analyzing a ligand-binding reaction, such as that between the myosin heads in the fibers and V_i, is to replot the data using a Hill plot (Fersht, 1985). Fig. 5 shows a Hill plot of isometric tension at 25°C as a function of $[V_i]$. The data were for fibers activated in the presence of 5 mM P_i, similarly to those shown in Fig. 2. The line fitted to the points by linear regression had a slope, equal to the Hill coefficient, of 0.99 (range, 0.88–1.31, 95% confidence limits). A Hill coefficient of 1.0 indicates that the ligand binds to a single type of site, all of which have the same free energy change upon binding. Thus the data indicate that there was no cooperativity between the heads for the trapping of the V_i ligand on myosin heads in fast-twitch skinned fibers. A similar plot was obtained in the presence of 50 mM P_i with a Hill coefficient of 0.81 (range, 0.68–0.93, 95% confidence limits). A Hill plot of the data shown in Fig. 4, obtained at 5°C, had a Hill coefficient of 0.82, (range, 0.70–0.94, 95% confidence limits). Although the Hill coefficients obtained under the different conditions were slightly different, statistically the curves were not significantly different from each other at the 95% confidence level.

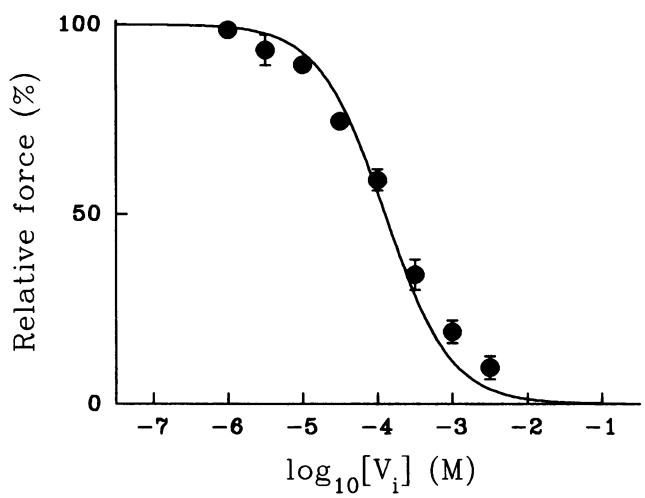

FIGURE 4 Data points show relative maximally Ca^{2+}-activated isometric force vs. $\log_{10}[V_i]$ in the presence of P_i (5 mM) similar to that shown in Fig. 2 with the exception that the temperature was lowered to 5°C. Relative force was determined by comparing the force obtained during activation in the presence of V_i and P_i (5 mM) to that obtained either before or after this when fibers were activated in the absence of V_i and in the presence of P_i (5 mM). Bars represent SEM ($3 \leq n \leq 5$ fibers for each data point). The curve is that for a simple binding isotherm with a Hill coefficient of 1, where $P/P_o = 100(1 - ([Vi]/K_d + [Vi]))$, in which P/P_o is the relative force (%) and the dissociation constant, K_d, was determined from a regression line (fitted to the data at $[V_i] \geq 10^{-5.0}$ M) to be $10^{-3.9}$ M $[V_i]$. The binding isotherm was not fit to the data but rather was calculated to show that the data do not deviate significantly from this curve.

MgATPase activity

It was expected that the MgATPase activities of Ca^{2+}-activated muscle fibers and actin-activated myosin would differ, since isolated contractile proteins are not subject to

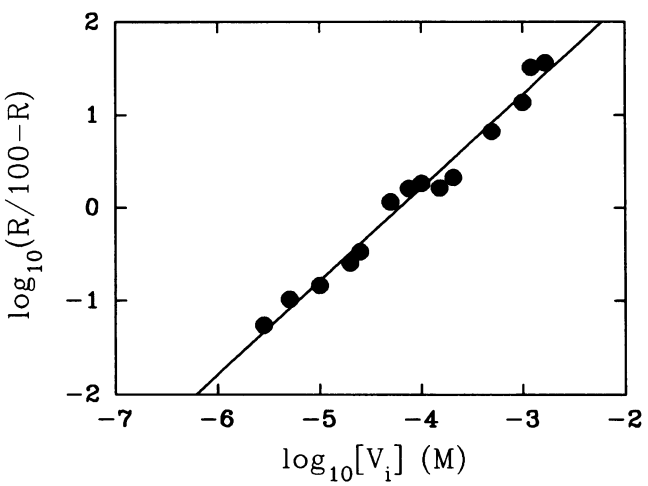

FIGURE 5 Hill plot of data obtained from the inhibition of force in fast-twitch fibers in the presence of various concentrations of V_i. Data points are taken from skinned fibers activated under similar conditions to those shown in Fig. 2 in the presence of P_i (5 mM). Data were calculated using the equation $Y = \log_{10}(R/100 - R)$ for the ordinate, where R is the proportion (%) of heads trapped by V_i (100 minus the proportion generating force). This was plotted against the $\log_{10}[V_i]$. The correlation coefficient for the line of best fit was $r = 0.99$. Values obtained using $[V_i]$ that were below the threshold for force inhibition were not included because inaccuracies in these values often distort Hill plots (Fersht, 1985).

steric constraints as are the proteins in the intact contractile apparatus. We were therefore interested to compare the effects of V_i upon the MgATPase activity in intact Ca^{2+}-activated fast-twitch fibers and in an actin-activated myosin-S1 system, since S1 is the myosin species least likely to be affected by steric constraints. Such data would give information about the energetics of different cross-bridge states.

Results in Fig. 6 show that the MgATPase activity of fast-twitch fibers was inhibited with a similar dependence upon $[V_i]$ as was force generation. The rate of P_i production was determined by sampling fiber-activating solutions at 1, 2, and 3 min following Ca^{2+}-activation. P_i production by fibers was linear, with 21.5 ± 4.0 nmol P_i produced per mg of myosin per second (mean ± SEM, n = 6 fiber bundles) in the absence of V_i. Tension measurements made in parallel with fibers from the same fiber bundle under similar conditions (omitting added P_i) showed that tension remained high during the measurement with relative maximally Ca^{2+}-activated force levels of (P/P_o) = 99 ± 2%, 97 ± 2% and 91 ± 4% (mean ± SEM, n = 3) at 1, 2, and 3 min, respectively, after maximal Ca^{2+} activation. The fibers produced a maximum tension of 23 ± 12 N/cm^2 (mean ± SEM, n = 3). Although some sarcomere inheterogeneity appears in this preparation over this length of time, it is unlikely that it would alter the basic conclusion drawn below, that MgATPase activity is inhibited in parallel with tension. The maximal rate of fiber MgATPase activity at 25°C was 4.95 ± 0.90 mol of ATP hydrolyzed s^{-1} per mole of myosin heads (mean ± SEM, n = 6 fiber bundles). Values obtained in other laboratories under similar conditions have been close to this. Webb et al. (1986) and Kawai et al. (1987) obtained values for MgATP hydrolysis of 3.2 and 3.0 s^{-1} per myosin head, respectively, in skinned rabbit fast-twitch fibers. A value of 3.82 s^{-1} per myosin head was obtained for skinned rat skeletal muscle fibers at 21–22°C (Stephenson et al., 1989). At a temperature of 5°C, at which sarcomere heterogeneity is better maintained, an activity of 0.98 s^{-1} was found for rabbit fast-twitch fibers by Brenner (1988). This value also agrees well with ours if one assumes a Q_{10} for MgATPase activity of 2.1, which was that determined for the maximum velocity of rabbit psoas fiber shortening over a similar temperature range (Pate et al., 1994).

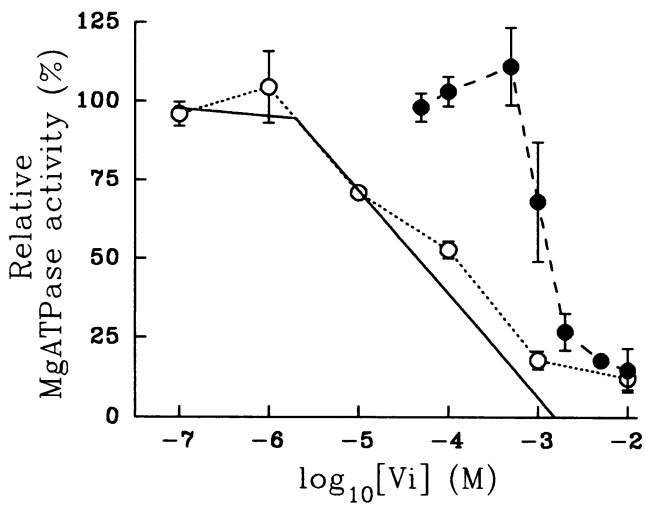

FIGURE 6 The effects of V_i upon relative MgATPase activity for rabbit fast skeletal muscle myosin S1 (18 μg ml^{-1}) activated in the presence of F-actin (1 mg ml^{-1}) (●, each data point $2 \leq n \leq 4$ observations, from a total of 6 acto-S1 preparations), and upon relative maximally Ca^{2+}-activated MgATPase activity for rabbit fast-twitch muscle fibers (○, each data point $3 \leq n \leq 5$ observations from a total of 5 fiber bundles). Results are means ± SEM. MgATPase activity was measured using a malachite green method for the determination over time of P_i production from the hydrolysis of MgATP. The *solid line* is the curve fitted to the data for the decline of force in fast-twitch fibers due to increasing $[V_i]$ in the presence of 5 mM P_i taken from Fig. 2, and is included here for easy comparison.

The maximal MgATPase activity remained fairly stable until $[V_i]$ reached ~1 μM and then declined linearly with the $\log_{10}[V_i]$ from its maximal to its minimal levels with an $\sim 10^{2.4}$-fold increase in $[V_i]$. The MgATPase activity in the presence of 10 mM V_i, a $[V_i]$ at which force was not detectable, remained at 0.17 ± 0.05 s^{-1} per myosin head (mean ± SEM, n = 5). This indicates that there was a Ca^{2+}-activated rate of MgATPase activity of 12% of maximal which could not be abolished by V_i. This rate is limited by the rate of release of V_i from an actomyosin complex.

Since the MgATPase activity of fast-twitch fibers was not completely inhibited even by concentrations of V_i that abolished force generation, this indicates that although trapping the myosin heads using V_i prevents force generation, the cross-bridge cycle continues due to the release of V_i. Thus during Ca^{2+} activation in the presence of V_i the trapped heads are in a steady state. The rate of cross-bridge cycling, 0.17 s^{-1}, should be similar to the rate of V_i release measured by the recovery of tension following activation in MgATP (Fig. 1). Tension recovers with a first order rate of ~0.08 s^{-1}. These two rates differ by only a factor of two.

The maximal MgATPase activity of acto-S1 in the presence of an F-actin concentration of 1 mg ml^{-1} was 0.36 ± 0.07 mol P_i generated per mol S1 s^{-1} (mean ± SEM, n = 6). The MgATPase activity of the fibers was 20-fold more sensitive to V_i trapping than the MgATPase activity of acto-S1. Therefore, the steric constraints imposed by the intact contractile apparatus alter the V_i trapping reaction. However, the effect is not as great as might be expected for some models of this interaction (see Discussion).

DISCUSSION

The dependence of force on V_i concentration

We have measured the dependence of force upon vanadate concentration in the presence of two well defined concentrations of inorganic phosphate. We found that force declined linearly with $\log_{10}[V_i]$, as has been found previously for P_i by Pate and Cooke (1989b) and by Millar and Homsher (1990). However, unlike the case for P_i, the force did not continue to increase as $[V_i]$ decreased. In addition, the high affinity of V_i for the active site of myosin (Goodno, 1982) allowed the tension to be titrated to 0, thereby defining the

entire curve. Although the decline in tension shown in Fig. 2 can be fitted well by straight lines, the data are not statistically significantly different from the behavior expected for a simple binding isotherm. In particular, an increase in $[V_i]$ of about $10^{2.8}$-fold to $10^{3.0}$-fold is required to reduce the force from 100% to 0%. Similar values were obtained in the presence of 5 mM P_i, 50 mM P_i, or 50 μM AlF_x, and at two temperatures (5 and 25°C) (Figs. 2–4). The data, when analyzed in a Hill plot, display a slope that is close to unity, characteristic of the binding of a ligand to a simple non-cooperative site on a protein (Fig. 5). This observation has several implications for models of cross-bridge energetics, discussed below.

V_i as a probe of force generating states

The dependence of tension upon $[V_i]$ provides information on the energetics of the transition involving V_i binding. The analysis is analogous to the case for the binding of P_i, previously discussed by Pate and Cooke (1989a). The main differences are that force can be titrated to very low levels and variation in $[V_i]$ does not alter the free energy change of ATP hydrolysis.

As the concentration of V_i increases, the free energies of the actin·myosin·ADP·V_i and myosin·ADP·V_i states decrease relative to the corresponding actin·myosin·ADP·P_i and myosin·ADP·P_i states. For example, for myosin heads near the beginning of the power stroke the free energy would be high, similar to that of the actin·myosin′·ADP state depicted in Fig. 7. For the free energy depicted in Fig.7 for the actin·myosin·ADP·V_i state, corresponding to a moderate concentration of V_i, the binding of V_i to the actin·myosin·ADP state would be favorable. However, for those states that have a lower free energy, such as that of the actin·myosin·ADP state shown in Fig. 7, a much larger concentration of V_i is required before the binding of V_i would be favorable. Thus the range of concentrations of V_i required to titrate force to 0 provides a measure of the range of free energies of the states to which the V_i is binding.

The classical method for analyzing the energetics of the binding of a ligand to a protein is the Hill equation (Fersht, 1985). The Hill plot of the decrease in tension shown in Fig. 5 has a slope close to 1.0, and thus follows the behavior expected for a simple isotherm obtained from the binding of a ligand non-cooperatively to a protein. That is to say, the protein sites to which the ligand V_i is binding all have the same free energy. The slopes of the Hill plots ranged from 1.0 to 0.8 under a variety of conditions. A value of 0.8 suggests that the free energies of the actin·myosin′·ADP states are distributed over a modest range. To investigate how the relationship between force and $\log_{10}[V_i]$ depends on the free energies of the actin·myosin′·ADP states, the data expected for several cases were plotted in Fig. 8. The free energies of the theoretical actin·myosin′·ADP states are distributed evenly over four different ranges, with the widths of the ranges being 0, 4.6, 9.2, and 15.0 kT (where k is Boltzmann's constant, T is the temperature, and kT is the thermal energy,

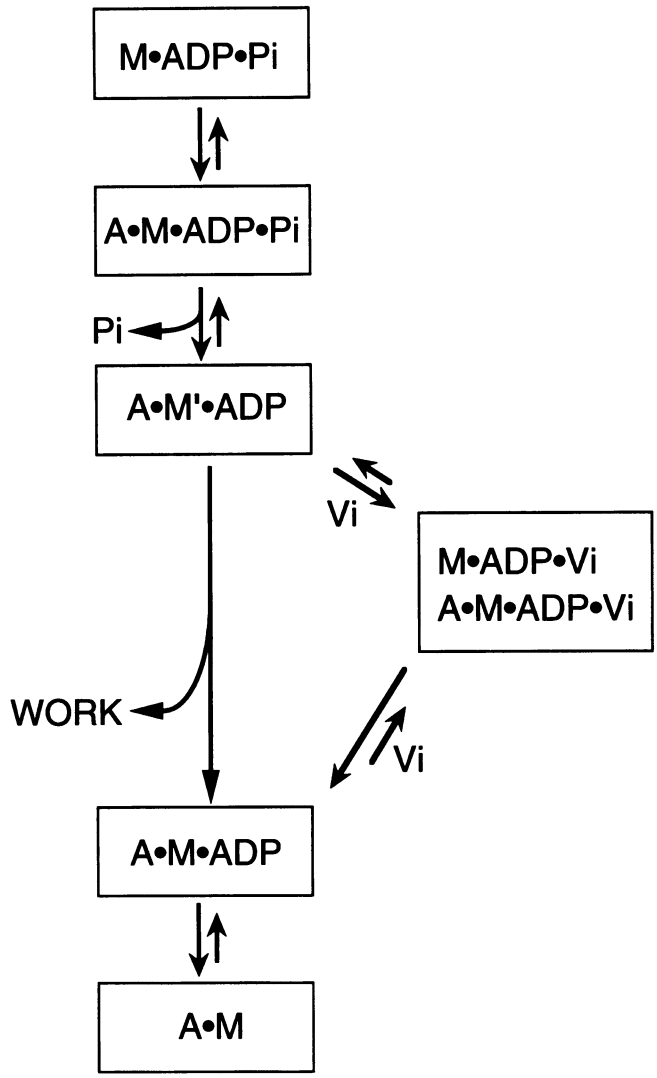

FIGURE 7 Model showing structural states of the cross-bridge cycle involved in binding of P_i and V_i. The vertical position of the states in the diagram represents their approximate free energies. The release of P_i from A·M·ADP·P_i leads to a state A·M′·ADP. This transition is thought to occur near the beginning of the power stroke where the free energy of the A·M′·ADP state is high. Subsequent isomerizations result in a large drop in free energy, which is converted to mechanical work in a contracting fiber, leading to the state A·M·ADP. This state has a low free energy, represented by a lower vertical position in the diagram, and it represents the conformation at the end of the power stroke. V_i also binds to A·M′·ADP leading to A·M·ADP·V_i which dissociates rapidly to M·ADP·V_i. The free energy of the vanadate states is shown such that binding of V_i would be favorable to A·M′·ADP, but would not be favorable to A·M·ADP, which has a much lower free energy.

equal to ~2.5 kJ/mol at 283 K). As the free energies of these states are distributed over an increasing range, the slope of the force vs. $\log_{10}[V_i]$ plot becomes more shallow. The data from Fig. 4 obtained at 5°C, with a Hill coefficient of 0.82, are also plotted in Fig. 8 for comparison. These data are best fit by a model in which the free energies of the actin·myosin′·ADP states are distributed over ~3.5 kT. However, at the 90% confidence level, the data are not statistically significantly different from the curve for binding to

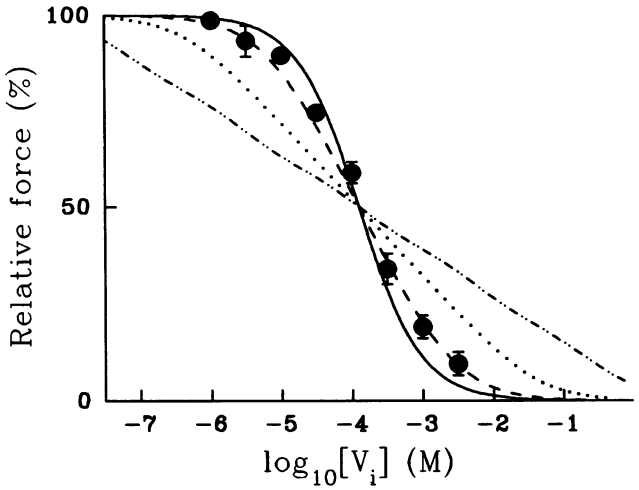

FIGURE 8 The effect of distributing the free energies of the A·M′·ADP states through a range of values. The tension expected for the binding of V_i to a series of A·M′·ADP states was simulated using a variation of the model shown in Fig. 7. The A·M′·ADP state could bind Vi to form a non-force A·M·ADP·V_i state (as shown by the double arrows connecting these states). Those states that did not bind V_i continued through the cycle to force-producing states, A·M·ADP in Fig. 7, and tension was taken as proportional to the population of these states. These force-producing states were assumed to not bind to Vi, omitting the transitions shown by the lower double arrows connecting these states. The transitions between the A·M′·ADP and A·M·ADP·V_i were assumed to occur faster than steady state cycling. However, the results were not altered greatly when the rate of cycling through the states was assumed to be equivalent to the rate of binding of Vi. A higher cycling rate required a higher concentration of V_i in order to affect tension, but it did not change the shape of the relation between force and $[V_i]$. The curve with the steepest slope (*solid line*) was simulated assuming that the free energy of A·M′·ADP was a single value. This curve is the same as that shown in Fig. 4, representing a simple binding isotherm with the single value of K_d defined in Fig. 4 ($10^{-3.9}$ M V_i). The curve with the next steepest slope (*dashed line*) was simulated assuming that the A·M′·ADP states were distributed across a range of 4.6 *kT*, with K_d distributed across 2 $\log_{10}[V_i]$ units. The curve with the *dotted line* was for a range of 9.2 *kT* with K_d distributed across 4 $\log_{10}[V_i]$ units, and the shallowest curve (*dashes and dots*) was for a range of 15 *kT* with K_d distributed across 6.5 $\log_{10}[V_i]$ units. This curve is that expected if the A·M′·ADP state was the major force-generating state, and it is similar to that calculated by Pate and Cooke (1989) using a more complex model.

a single site. The data shown would allow at most a distribution over 5 *kT*.

Models of force generation

Many models of cross-bridge function predict that the state(s) involved in the power stroke would have free energies that would be distributed over a considerable range. These states are thought to involve the ternary complex, actin·myosin·ADP. In the discussion below we show that if V_i inhibits tension by binding to these force producing states the slope of the force vs. $\log_{10}[V_i]$ plot would be more shallow than the one we obtained (Fig. 8). In contrast our data suggest a simple transition between two states separated by a single value of free energy (or at most a small range of free energies).

The kinetics and energetics of the interactions between actomyosin and nucleotides have been studied extensively both using purified proteins in solution and using muscle fibers (for reviews see Taylor, 1979; Sleep and Smith, 1981; Cooke, 1986; Hibberd and Trentham, 1986; Goldman and Brenner, 1987; Geeves, 1991). These studies have suggested that myosin·ADP·P_i forms a weak bond with actin at the beginning of the power stroke. The resulting state, actin·myosin·ADP·P_i, generates little force and thus has a free energy that is not strongly dependent on the position of actin (Fig. 7). Following the release of P_i from the actin·myosin·ADP·P_i complex, force is developed by a state in which the free energy depends strongly on the position of the actin relative to the myosin to which it is attached. The transition to the force generating state occurs at the beginning of the power stroke to a state in which the actin·myosin·ADP bond is still weak, denoted by actin·myosin′·ADP in Fig. 7. Further transitions result in a large drop in free energy, leading to states in which the myosin is bound strongly to actin at the end of the power stroke, denoted by actin·myosin·ADP in Fig. 7. In the filament array of the fiber, steric constraints will dictate that myosin interacts with actin in a variety of relative positions. Thus one would expect the force producing actin·myosin·ADP states in active fibers to be separated by different amounts of free energy for different myosin heads. One can estimate the drop in free energy between the beginning and end of the power stroke to be of the order of 15 *kT*, ~60% of the energy available from one ATP. We show that V_i does not bind to states that have such a large spread in free energies, and thus it does not bind directly to the force-generating states.

The dependence of force upon $[V_i]$ provides a probe of the energetics of the cross-bridge states to which V_i binds. As $[V_i]$ increases, the free energies of the states with bound V_i decrease, allowing V_i to bind to actin·myosin·ADP states with increasingly negative free energies (Fig. 7). If V_i binds directly to force-producing states, the change in the $[V_i]$ required to bind to all of these states would be large, as discussed by Pate and Cooke (1989a, b) for the binding of P_i. The inhibition of force by V_i would begin to occur when the free energy of the V_i states reached that of the actin·myosin′·ADP state at the top of the power stroke but inhibition would not be complete until the free energy of the V_i states reached that of the actin·myosin·ADP states at the end of the power stroke. To move through 15 *kT* in free energy the concentration of $[V_i]$ would have to increase by more than 6 orders of magnitude (shallowest curve in Fig. 8), rather than the 2.8–3.0 orders of magnitude observed (data points in Fig. 8).

In view of the expected complexity of the actomyosin and nucleotide binding interactions, it is unexpected that the Hill plot has a slope close to 1.0 (Fig. 5), that expected for a simple transition between two states separated by a single value of free energy. If the binding of V_i to myosin involved a transition that was strongly influenced by myofilament lattice constraints, such a simple isotherm would not result. In addition, if the actin·myosin·ADP states were distributed

over a range of free energies we would also expect the competition of V_i with other ligands, P_i or AlF_x, to alter the slope of the force vs. $\log_{10}[V_i]$ relation. As the concentration of the competing ligand is raised it will bind first to the actin·myosin·ADP states with higher free energies, leaving only those with lower free energies available for binding of V_i. Thus in the presence of a competing ligand the slope of the force vs. $\log_{10}[V_i]$ relation would be steeper. In contrast we find that the slope is unchanged, even in the presence of ligands that have lowered force by 25–75%.

We conclude that the actin·myosin·ADP states to which V_i binds are distributed over a modest range of free energies, 0–5 *kT*. Two models could fit this data. In one model, the actin·myosin′·ADP state to which V_i binds is a weakly bound state, with a free energy profile that is similar to the actin·myosin·ADP·P_i or actin·myosin·ADP·V_i states. In the second model the actin·myosin′·ADP is a force- generating state. However, the cross-bridges would all be distributed near the beginning of the power stroke. The data in Fig. 6, as well as a number of results obtained by other investigators, all support the first of the two models, as discussed below. However, the exact constraints placed on cross-bridge models by the observation of a single isotherm will require a more detailed analysis.

Inhibition of acto-S1 MgATPase

The magnitude of the difference in concentrations of V_i required to inhibit the MgATPase activities of fibers and of contractile proteins in solution (Fig. 6) is also not easily explained by models in which the transition to force generation is directly coupled to the release of P_i. The concentration of V_i required to produce one-half inhibition is directly related to the concentration of the actin·myosin′·ADP state(s) to which it binds. The concentration of this state is expected to be much higher in fibers, where steric constraints will prevent the head from rotating. Head rotation is required to reach the states of lower free energy nearer the end of the power stroke. In contrast, the concentration of the actin·myosin′·ADP state(s) are expected to be lower during steady state hydrolysis by acto-S1, because there are no steric constraints to retain the head in a highly strained position. If the actin·myosin′·ADP state is a highly strained, force-producing state, the release of P_i from an acto-S1 complex in solution would involve almost immediate rotation of the myosin head to its free energy minimum (actin·myosin·ADP in Fig. 7). The observation that the concentration of Vi required to inhibit the acto-S1 ATPase is only 20 times greater than required to inhibit fibers shows that the concentration of the actin·myosin′·ADP state(s) is appreciable. An appreciable population can only occur if this state is not highly strained leading to a rapid transition to the end of the power stroke. Thus the data require that the actin·myosin′·ADP state to which Vi binds is not highly strained. A similar phenomenon is seen for the binding of P_i. The rate of P_i exchange into ATP in fibers is ~500 times faster than that for acto-S1 (Bowater and Sleep, 1988), a result that was also explained by the existence of an unstrained actin·myosin′·ADP state with a high free energy relative to the actin·myosin·ADP state.

Inhibition of force by P_i

Fiber tension can also be inhibited by addition of P_i, although complete inhibition of tension cannot be achieved at concentrations of P_i which maintain physiological ionic strength. To compare the inhibition of force by P_i with the inhibition by V_i, data from a number of studies were pooled and are plotted in Fig. 9 along with a curve fit to the data for the inhibition of force by V_i in the presence of 5 mM P_i. Plotted in this way, the slope of the line through the P_i data (−41.4, spanning 2.42 $\log_{10}[P_i]$ units from 100% to 0% force) is a little steeper than the one through the V_i data (a slope of −36 to −33, spanning 2.8–3.0 $\log_{10}[V_i]$). A major difference between V_i and P_i is the weaker binding of P_i, evidenced by a shift of the curve to the right. The data suggest that the K_d for V_i binding (Fig. 4) is about 127-fold higher than the K_d for P_i binding, which is why it is possible to titrate force to 0 at physiological ionic strength using V_i. A second major differences between V_i and P_i is the fact that tension continues to rise as the concentration of P_i is lowered below 5 mM. The continued rise in tension may reflect the increased free energy available from ATP at the lower concentrations of P_i. However, if P_i inhibits tension by binding to the same actin·myosin′·ADP state as does V_i, then one would expect the same dependence of force upon ligand concentration, and

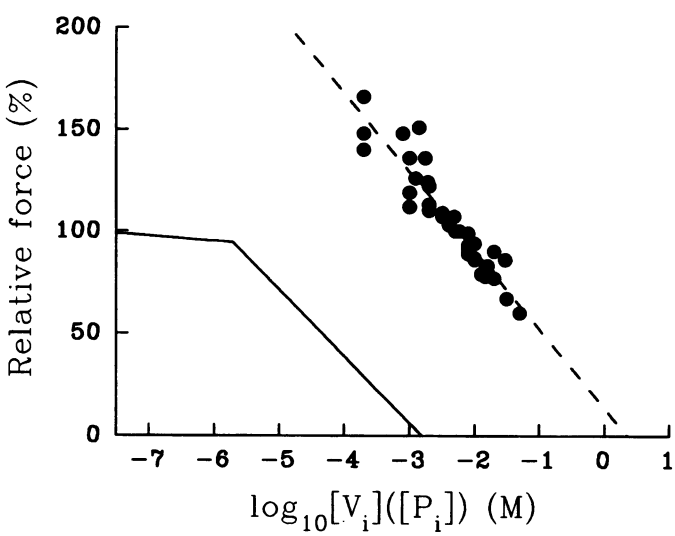

FIGURE 9 The inhibition of force by P_i in fast-twitch skeletal muscle fibers is compared to inhibition by V_i. The *circles* represent data for inhibition by P_i taken from several sources (Altringham and Johnston, 1985 (Antarctic fish); Kawai et al., 1987 (rabbit psoas); Pate and Cooke, 1989b (rabbit psoas, pH 7.0, 5 mM ATP); Millar and Homsher, 1990 (rabbit psoas); Kawai and Halvorson, 1991 (rabbit psoas); Dantzig et al., 1992 (rabbit psoas, 12°C); Martyn and Gordon, 1992 (rabbit psoas)). Each set of data was normalized by setting the tension obtained in the presence of 5 mM P_i to 100%. The *dashed line* was fit by linear regression (r = 0.96). The *solid line* is the fit to the data in Fig. 2 of this manuscript for inhibition by V_i in the presence of 5 mM P_i.

the drop in force should occur over a range of about 3 $\log_{10}$-$[P_i]$ units. A fit of a straight line to the P_i inhibition data shown in Fig. 9 intercepts the abscissa at +0.13 ($10^{0.13}$ M P_i), suggesting that force should reach a plateau as $[P_i]$ decreases below 1 mM ($10^{-3.0}$ M P_i). Although no strong tendency to plateau is evident in the data, there are only three data points below 1 mM $[P_i]$, and these are difficult points to obtain because they require the use of the P_i scavenger sucrose phosphorylase to lower $[P_i]$ (Pate and Cooke, 1989b; Millar and Homsher, 1990; Martyn and Gordon, 1992). If the data were to reach a plateau at $[P_i]$<0.2 mM, the lowest $[P_i]$ shown in Fig. 9, then the inhibition of force by P_i would follow approximately the same concentration dependence as observed for V_i with a midpoint at ~16 mM P_i. This midpoint defines a dissociation constant, K_d, for P_i in active fast-twitch fibers of ~16 mM. This value is similar to the value of 6–12 mM determined from studies of the force transients observed following release of caged P_i at 12–15°C (Dantzig et al., 1992; Walker et al., 1992), and it is not far from the K_m of 3 mM found for the exchange of P_i into ATP (Bowater and Sleep, 1988).

We conclude that the data are consistent with P_i binding to an actin·myosin′·ADP state that is not force-producing. The data suggest that the free energy of this state is approximately that of the actin·myosin·ADP·P_i state at 16 mM $[P_i]$. Thus this transition is almost isoenergetic at physiological $[P_i]$ in active fibers, leading to efficient energy transduction. As $[P_i]$ rises during fatigue, the actin·myosin·ADP·P_i state would decrease in free energy, and fewer cross-bridges would make the transition to the actin·myosin′·ADP state. However, those that did would generate the same mechanical work, helping to preserve efficiency as $[P_i]$ increases. A test of this hypothesis could be made by measuring tension at concentrations of P_i below 0.2 mM using more efficient P_i scavengers to determine whether force does reach a plateau.

The transition to a force-generating state

The data discussed above suggest that the actin·myosin′·ADP states to which V_i binds do not have the energetics expected for highly strained, force-producing states. The data are more easily explained by assuming a model in which the preferred orientation of myosin is not tightly coupled to the state of the nucleotide. Thus the transition between actin·myosin′·ADP and actin·myosin′·ADP·V_i does not involve conformational changes that are linked to force generation. Force is generated after an isomerization between unstrained (actin·myosin′·ADP) and highly strained (actin·myosin·ADP) states and is not coupled directly to the state of the nucleotide. A similar uncoupling of nucleotide state and force generation has been proposed to explain the tension transients which follow photolytic release of P_i in isometrically contracting Ca^{2+}-activated fibers (Millar and Homsher, 1990; Dantzig et al., 1992; Walker et al., 1992). The data of Dantzig and co-workers was best explained by an isomerization that preceded P_i release, while Walker and co-workers concluded that the isomerization could also follow P_i release. The observation of a simple isotherm for force inhibition is compatible with isomerizations that precede or follow P_i release. The data of Fig. 6 would suggest that an isomerization should follow P_i release. Geeves (1991) has also invoked multiple structural states of the contractile proteins for each state of the bound nucleotide to explain the kinetics of the acto-S1 interaction in solution. A more extensive set of simulations for the two cases is now under way to determine more precisely which models can best fit the data.

We thank John Paige, Janet Daijo, and Jack Maypole for technical assistance with collection of data in some figures, and Michael Isard for assistance with modifications to the software used to collect data. We also thank Drs. Ed Pate and Christine Cremo for helpful discussions. Kathy Franks-Skiba and Dr. Brett Hambly kindly prepared the myosin and actin used.

This work was supported by U.S. Public Health Service grant AM30868, by a Neuromuscular Disease Research Fellowship to G.J.W. from the Muscular Dystrophy Association of America, and by a grant-in-aid from the Muscular Dystrophy Association of America to R.C.

REFERENCES

Altringham, J. D., and I. A. Johnston. 1985. Effects of phosphate on the contractile properties of fast and slow muscle fibres from an Antarctic fish. *J. Physiol. (Lond.).* 368:491–500.

Bowater, R., and J. Sleep. 1988. Demembranated muscle fibers catalyze a more rapid exchange between phosphate and adenosine triphosphate than actomyosin subfragment 1. *Biochemistry.* 27:5314–5323.

Brenner, B. 1988. Effect of Ca^{2+} on cross-bridge turnover kinetics in skinned single rabbit psoas fibers: implications for regulation of muscle contraction. *Proc. Natl. Acad. Sci. USA.* 85:3265–3269.

Chase, P. B., and M. J. Kushmerick. 1988. Effects of pH on contraction of rabbit fast and slow skeletal muscle fibers. *Biophys. J.* 53:935–946.

Chase, P. B., D. A. Martyn, M. J. Kushmerick, and A. M. Gordon. 1993. Effects of inorganic phosphate analogs on stiffness and unloaded shortening of skinned muscle fibres from rabbit. *J. Physiol. (Lond.).* 460: 231–246.

Cooke, R. 1972. A new method for preparing myosin subfragment-1. *Biochem. Biophys. Res. Commun.* 49:1021–1028.

Cooke, R. 1986. The mechanism of muscle contraction. *CRC Crit. Rev. Biochem.* 21:53–118.

Cooke, R., and K. E. Franks. 1978. Generation of force by single-headed myosin. *J. Mol. Biol.* 120:361–373.

Cooke, R., K. Franks, G. B. Luciani, and E. Pate. 1988. The inhibition of rabbit skeletal muscle contraction by hydrogen ions and phosphate. *J. Physiol. (Lond.).* 395:77–97.

Cremo, C. R., J. C. Grammer, and R. G. Yount. 1989. Direct chemical evidence that serine 180 in the glycine-rich loop of myosin binds to ATP. *J. Biol. Chem.* 264:6608–6611.

Dantzig, J. A., and Y. E. Goldman. 1985. Suppression of muscle contraction by vanadate: mechanical and ligand binding studies on glycerol-extracted rabbit fibers. *J. Gen. Physiol.* 86:305–327.

Dantzig, J. A., Y. E. Goldman, N. C. Millar, J. Lacktis, and E. Homsher. 1992. Reversal of the cross-bridge force-generating transition by photogeneration of phosphate in rabbit psoas muscle fibres. *J. Physiol. (Lond.).* 451:247–278.

Fersht, A. 1985. Enzyme Structure and Mechanism, 2nd ed. Freeman, New York. 263–292.

Fuchs, F. 1985. The binding of calcium to detergent-extracted rabbit psoas muscle fibres during relaxation and force generation. *J. Muscle Res. Cell Motil.* 6:477–486.

Geeves, M. A. 1991. The dynamics of actin and myosin association and the crossbridge model of muscle contraction. *Biochem. J.* 274:1–14.

Goldman, Y. E., and B. Brenner. 1987. Special topic: molecular mechanism of muscle contraction. *Annu. Rev. Physiol.* 49:629–635.

Goodno, C. C. 1982. Myosin active site trapping with vanadate ion. *Methods Enzymol.* 85:116–123.

Goody, R. S., W. Hofmann, M. K. Reedy, A. Magid, and C. Goodno. 1980. Relaxation of glycerinated insect flight muscle by vanadate. *J. Muscle Res. Cell Motil.* 1:198–199.

Grammer, J. C., and R. G. Yount. 1994. A proposed mechanism for the vanadate moderated cleavage of myosin. *Biophys. J.* 66:77*a*. (Abstr.).

Gresser, M. J., A. S. Tracey, and K. M. Parkinson. 1986. Vanadium (V) oxyanions: the interaction of vanadate with pyrophosphate, phosphate, and arsenate. *J. Am. Chem. Soc.* 108:6229–6234.

Herzig, J. W., J. W. Peterson, J. C. Rüegg, and R. J. Solaro. 1981. Vanadate and phosphate ions reduce tension and increase cross-bridge kinetics in chemically skinned heart muscle. *Biochim. Biophys. Acta.* 672:191–196.

Hibberd, M. G., J. A. Dantzig, D. R. Trentham, and Y. E. Goldman. 1985. Phosphate release and force generation in skinned muscle fibers. *Science.* 228:1317–1319.

Hibberd, M. G., and D. R. Trentham. 1986. Relationships between chemical and mechanical events during muscular contraction. *Annu. Rev. Biophys. Biophys. Chem.* 15:119–161.

Kawai, M., K. Güth, K. Winnikes, C. Haist, and J. C. Rüegg. 1987. The effect of inorganic phosphate on the ATP-hydrolysis rate and the tension transients in chemically skinned rabbit psoas fibers. *Pflügers Arch.* 408: 1–9.

Kawai, M., and H. R. Halvorson. 1991. Two step mechanism of phosphate release and the mechanism of force generation in chemically skinned fibers of rabbit psoas muscle. *Biophys. J.* 59:329–342.

Kentish, J. C. 1986. The effects of inorganic phosphate and creatine phosphate on force production in skinned muscles from rat ventricle. *J. Physiol. (Lond.).* 370:585–604.

Kodama, T., K. Fukui, and K. Kometani. 1986. The initial phosphate burst in ATP hydrolysis by myosin and subfragment-1 as studied by a modified malachite green method for determination of inorganic phosphate. *J. Biochem.* 99:1465–1472.

Lymn, R. W., and E. W. Taylor. 1971. Mechanism of adenosine triphosphate hydrolysis by actomyosin. *Biochemistry.* 10:4617–4624.

Margossian, S. S., and S. Lowey. 1982. Preparation of myosin and its subfragments from rabbit skeletal muscle. *Methods Enzymol.* 85:55–71.

Martyn, D. A., and A. M. Gordon. 1992. Force and stiffness in glycerinated rabbit psoas fibers: effects of calcium and elevated phosphate. *J. Gen. Physiol.* 99:795–816.

Mihashi, K., A. Ooi, and T. Hiratsuka. 1990. Evidence for the existence of two equilibrium conformations of the ternary complex of myosin subfragment-1, ADP, and orthovanadate. *J. Biochem.* 107:464–469.

Millar, N. C., and E. Homsher. 1990. The effect of phosphate and calcium on force generation in glycerinated rabbit skeletal muscle fibers. A steady state and transient kinetic study. *J. Biol. Chem.* 265:20234–20240.

Pate, E., and R. Cooke. 1989a. A model of crossbridge action: the effects of ATP, ADP and P_i. *J. Muscle Res. Cell Motil.* 10:181–196.

Pate, E., and R. Cooke. 1989b. Addition of phosphate to active muscle fibers probes actomyosin states within the power stroke. *Pflügers Arch.* 414: 73–81.

Pate, E., G. J. Wilson, M. Bhimani, and R. Cooke. 1994. Temperature dependence of the inhibitory effects of orthovanadate on shortening velocity in fast skeletal muscle. *Biophys. J.* In press.

Penningroth, S. M. 1986. Erythro-9-[3-(2-hydroxynonyl)]adenine and vanadate as probes for microtubule-based cytoskeletal mechanochemistry. *Methods Enzymol.* 134:477–487.

Rubinson, K. A. 1981. Concerning the form of biochemically active vanadium. *Proc. R. Soc. Lond. Ser. B. Biol. Sci.* 212:65–84.

Sleep, J. A., and R. L. Hutton. 1980. Exchange between inorganic phosphate and adenosine 5′-triphosphate in the medium by actomyosin subfragment 1. *Biochemistry.* 19:1276–1283.

Sleep, J. A., and S. Smith. 1981. Actomyosin ATPase and muscle contraction. *Curr. Top. Bioenerg.* 11:239–286.

Spudich, J. A., and S. Watt. 1971. The regulation of rabbit skeletal muscle contraction: biochemical studies of the interaction of the tropomyosin-troponin complex with actin and the proteolytic fragments of myosin. *J. Biol. Chem.* 246:4866–4871.

Stephenson, D. G., A. W. Stewart, and G. J. Wilson. 1989. Dissociation of force from myofibrillar MgATPase and stiffness at short sarcomere lengths in rat and toad skeletal muscle. *J. Physiol. (Lond.).* 410:351–366.

Taylor, E. W. 1979. Mechanism of actomyosin ATPase and the problem of muscle contraction. *CRC Crit. Rev. Biochem.* 7:103–164.

Taylor, E. W. 1991. Kinetic studies on the association and dissociation of myosin subfragment 1 and actin. *J. Biol. Chem.* 266:294–302.

Walker, J. W., Z. Lu, and R. A. Moss. 1992. Effects of Ca^{2+} on the kinetics of phosphate release in skeletal muscle. *J. Biol. Chem.* 267:2459–2466.

Webb, M. R., M. G. Hibberd, Y. E. Goldman, and D. R. Trentham. 1986. Oxygen exchange between P_i in the medium and water during ATP hydrolysis mediated by skinned fibers from rabbit skeletal muscle: evidence for P_i binding to a force generating state. *J. Biol. Chem.* 261: 15557–15564.

Weeds, A. G., and R. S. Taylor. 1975. Separation of myosin subfragment-1 isoenzymes from rabbit skeletal muscle myosin. *Nature.* 257:54–56.

Werber, M. M., Y. M. Peyser, and A. Muhlrad. 1992. Characterization of stable beryllium fluoride, aluminum fluoride, and vanadate containing myosin subfragment 1-nucleotide complexes. *Biochemistry.* 31:7190–7197.

White, D. C. S., and J. Thorson. 1972. Phosphate starvation and the nonlinear dynamics of insect fibrillar flight muscle. *J. Gen. Physiol.* 60: 307–336.

Wilson, G., J. Paige, and R. Cooke. 1990. Trapping spin-labeled ADP on myosin heads using vanadate. *Biophys. J.* 57:330a. (Abstr.).

Wilson, G., S. Shull, and R. Cooke. 1991. Myosin heads function independently during force generation. *Biophys. J.* 59:51a. (Abstr.).